Article

N-Alkyl Perfluoroalkanamides as Low Molecular-Mass Organogelators

Mathew George, Samuel L. Snyder, Pierre Terech, Charles J. Glinka, and Richard G. Weiss

J. Am. Chem. Soc., **2003**, 125 (34), 10275-10283• DOI: 10.1021/ja0362407 • Publication Date (Web): 05 August 2003

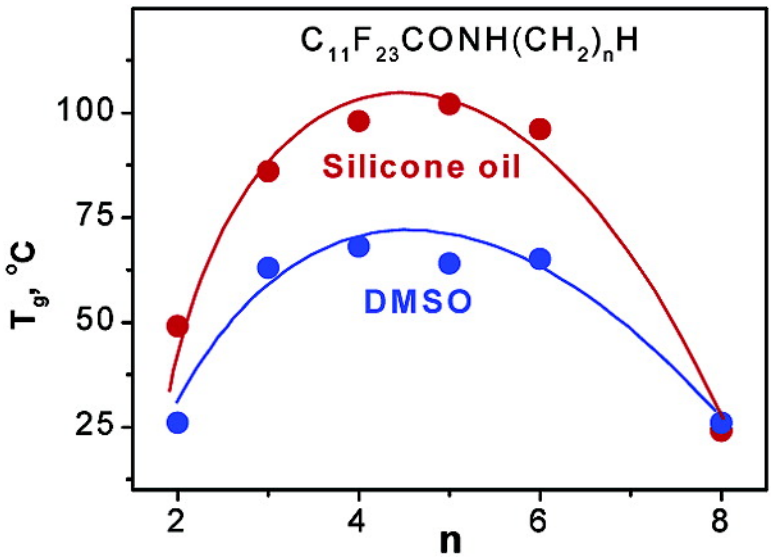

More About This Article

Additional resources and features associated with this article are available within the HTML version:

- Supporting Information
- Links to the 12 articles that cite this article, as of the time of this article download
- Access to high resolution figures
- Links to articles and content related to this article
- Copyright permission to reproduce figures and/or text from this article

View the Full Text HTML

J|A|C|S
ARTICLES
Published on Web 08/05/2003

N-Alkyl Perfluoroalkanamides as Low Molecular-Mass Organogelators

Mathew George,[†] Samuel L. Snyder,[†] Pierre Terech,[‡] Charles J. Glinka,[§] and Richard G. Weiss*,[†]

Contribution from the Department of Chemistry, Georgetown University, Washington, D.C. 20057-1227, Laboratoire Physico-Chimie Moleculaire, UMR 5819 CEA-Grenoble, 17 rue des Martyrs, 38054 Grenoble Cedex 09, France, and Center for Neutron Research, National Institute of Standards and Technology, Gaithersburg, Maryland 20899-8562

Received May 20, 2003; E-mail: weissr@georgetown.edu

Abstract: A new class of low molecular-mass organogelators (LMOGs), *N*-alkyl perfluoroalkanamides, $F(CF_2)_nCONH(CH_2)_mH$, is described. The molecules are designed to exploit the incompatibilities of their three molecular parts, and the results demonstrate that this strategy can be used to tune molecular aggregation and gel stability. The gelating properties of these LMOGs have been examined in a wide variety of organic liquids (including alkanes, alcohols, toluene, *n*-perfluorooctane, CCl_4, and DMSO) as a function of the *N*-alkyl and perfluoroalkyl chain lengths by X-ray diffraction, polarizing optical microscopy, infrared spectroscopy, differential scanning calorimetry, and small-angle neutron scattering (SANS). The gels are thermally reversible and require generally very low concentrations (<2 wt %) of LMOG. Several of the gels are stable for very long periods at room temperature. The incompatibility of the fluorocarbon and hydrocarbon segments causes the LMOGs to aggregate, probably into lamellae within the fibrils that constitute the basic unit of the gel networks. The SANS studies show that the cross-sections of fibers in the gel networks of LMOGs with shorter perfluoroalkyl chains are much larger than those with longer ones. Comparisons with the gelating properties of some analogous esters ($F(CF_2)_nCO_2(CH_2)_mH$) and diblock perfluoroalkylalkanes ($F(CF_2)_n(CH_2)_mH$) indicate that additional ordering within the aggregate units is enforced by the intermolecular H bonding among amide groups that is evidenced by IR spectroscopy. Analyses of these results and structure/solvent correlations are provided.

Introduction

Recently, interest in thermally reversible organogels, typically comprised of a small amount of a low molecular-mass organogelator (LMOG) and an organic liquid, and in the processes responsible for their formation has grown tremendously.[1−10] These gels contain microheterogeneous fibrillar phases that self-assemble in a wide variety of modes with structures expressed from the molecular to the micrometer distance scales. When sols or solutions of these systems are cooled below their characteristic gelation temperature (T_g), the LMOGs aggregate into fibers, strands, tapes, etc., joined at "junction zones" [6] to form networks that immobilize the liquid component, primarily by surface tension and capillary forces.[1,6] Since the organogelator concentration is usually very low, there need be no specific liquid-gelator interactions on the molecular scale. A model to describe the stages of aggregation in some organogels has been presented recently.[11]

Although LMOGs can be very simple molecules,[12,13] most have complex structures,[1,14,15] frequently with both lyophilic and hydrophilic or polar regions and several functional groups, or they are two-component systems that act via specific H-bonding interactions.[16] In addition, an exceedingly broad range of organic

[†] Georgetown University.
[‡] Laboratoire Physico-Chimie Moleculaire.
[§] National Institute of Standards and Technology.

(1) Terech, P.; Weiss, R. G. *Chem. Rev.* **1997**, *97*, 3133−3159.
(2) Abdallah, D. J.; Weiss, R. G. *Adv. Mater. (Weinheim, Ger.)* **2000,** *12*, 1237−1247.
(3) van Esch, J. H.; Feringa, B. L. *Angew. Chem., Int. Ed.* **2000**, *39*, 2263−2266.
(4) Shinkai, S.; Murata, K. *J. Mater. Chem*. **1998**, *8*, 485−495.
(5) Terech, P.; Weiss, R. G. In *Surface Characterization Methods*; Milling, A. J., Ed.; Marcel Dekker: New York, 1999; pp 286−344.
(6) Terech, P.; Furman, I.; Weiss, R. G. *J. Phys. Chem*. **1995**, *99*, 9558−9566.
(7) Partridge, K. S.; Smith, D. K.; Dykes, G. M. McGrail, P. T. *Chem. Commun.* **2001**, 319−320.
(8) Lu, L.; Cocker, M.; Bachman, R. E.; Weiss, R. G. *Langmuir* **2000**, *16*, 20−34.
(9) Ajayaghosh, A.; George, S. J. *J. Am. Chem. Soc*. **2001**, *123*, 5148−5149.
(10) Guan, L.; Zhao, Y. *J. Mater. Chem.* **2001**, *11*, 1339−1344.
(11) Aggeli, A.; Nyrkova, I. A.; Bell, M.; Harding, R.; Carrick, L.; McLeish, T. C. B.; Semenov, A. N.; Boden, N. *Proc. Natl. Acad. Sci. U.S.A.* **2001**, *98*, 11857−11862.
(12) Abdallah, D. J.; Weiss, R. G. *Langmuir* **2000**, *16*, 352−355.
(13) Abdallah, D. J.; Lu, L.; Weiss, R. G. *Chem. Mater*. **1999**, *11*, 2907−2911.
(14) Lu, L.; Weiss, R. G. *Chem. Commun.* **1996**, 2029−2030.
(15) Lin, Y.-C.; Kachar, B.; Weiss, R. G. *J. Am. Chem. Soc*. **1989**, *111*, 5542−5551.
(16) (a) Hanabusa, K.; Tange, J.; Taguchi, Y.; Koyama, T.; Shirai, H. *J. Chem. Soc., Chem. Commun*. **1993**, 390−392. (b) Hanabusa, K.; Miki, T.; Taguchi, Y.; Koyama, T.; Shirai, H. *J. Chem. Soc., Chem. Commun*. **1993**, 1382−1384. (c) Tomioka, K.; Sumiyoshi, T.; Narui, S.; Nagaoka, Y.; Iida, A.; Miwa, Y.; Taga, T.; Nakano, M.; Handa, T. *J. Am. Chem. Soc*. **2001**, *123*, 11817−11818. (d) Ahmed, S. A.; Sallenave, X.; Fages, F.; Mieden-Gundert, G.; Müller, W. M.; Müller, U.; Vögtle, F.; Pozzo, J.-L. *Langmuir* **2002**, *18*, 7096−7101. (e) Willemen, H. M.; Vermonden, T.; Marcelis, A. T. M.; Sudhölter, E. J. R. *Langmuir* **2002**, *18*, 7102−7106. (f) van der Laan, S.; Feringa, B. L.; Kellogg, R. M.; van Esch, J. *Langmuir* **2002**, *18*, 7136−7140.

liquids (including quasi-liquids such as supercritical CO_2[17]) and water[18] has been gelated. The unusual structural and diffusional properties of organogels have led to several interesting applications,[19−24] and they can be used as structure-directing agents for inorganic nanoparticles.[24a,25]

Here, we report that low concentrations of structurally simple *N*-alkyl perfluoroalkanamides, $F(CF_2)_nCONH(CH_2)_mH$, form very stable gels with a wide variety of organic liquids, including the first example of the gelation of a *n*-perfluoroalkane and other liquids that have been gelated by few other gelators. The molecular structures of these LMOGs contain "incompatible" segments: fluorocarbons and hydrocarbons are immiscible below a certain temperature, and the cross-sectional area of the $(CH_2)_n$ and $(CF_2)_n$ segments are 18.5 and 28.3 Å^2, respectively.[26] They are joined by an amide group whose intermolecular H-bonding interactions may enforce additional packing constraints.

Several other fluorinated gelators are known, but they are either more complex structurally or are much less efficient than the $F(CF_2)_nCONH(CH_2)_mH$. For instance, relatively high concentrations of related diblock molecules, (perfluoroalkyl)alkanes, are known to gelate several liquids,[27] including hydrocarbons[28] and mixtures of perfluorooctane and isooctane,[29] but not neat perfluorooctane.[28a] Hexafluorobenzene has been gelated by 12-hydroxyoctadecanoic acid,[30] and perfluorodecaline has been gelated by pentacosafluorodocosane ($F(CF_2)_{12}(CH_2)_{10}H$).[31] In the presence of ∼1−20% water, some partially fluorinated neutral and charged surfactants gelate a variety of liquids, including functionalized perfluoroalkanes.[32] Finally, some structurally complex, partially fluorinated aryl−alkyl amides and sugar derivatives have been shown to gelate a limited number of liquids.[33]

Scheme 1

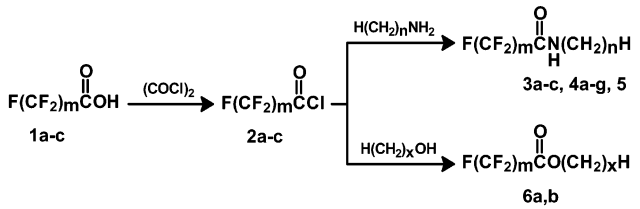

1a, **2a**, m = 7
1b, **2b**, m = 11
1c, **2c**, m = 17

3a, m = 7; n = 3
3b, m = 7; n = 10
3c, m = 7; n = 18

4a, m = 11; n = 0
4b, m = 11; n = 2
4c, m = 11; n = 3
4d, m = 11; n = 4
4e, m = 11; n = 5
4f, m = 11; n = 6
4g, m = 11; n = 8

5, m = 17; n = 3

6a, m = 11; x = 3
6b, m = 11; x = 18

We reasoned that insertion of an amide group between the alkyl and perfluoroalkyl portions of a (perfluoroalkyl)alkane would increase the strength of intermolecular interactions via H bonding[34] (since the secondary amide groups have a carbonyl group for H-bond acceptance and retain one H atom for donation) while retaining the segregation of packing between the molecular fragments. In fact, the use of amide groups is a common strategy to enhance the gelating ability of molecules.[16c,18a,35] It has allowed very low concentrations of some of the *N*-alkyl perfluoroalkanamides (**3**−**5**) in Scheme 1 to gelate a wide variety of organic liquids that includes one that has not been gelated previously (*n*-perfluorooctane), others that are gelated by only a few LMOGs (CCl_4 and DMSO), as well as aromatic molecules, alkanes, and alcohols. Here, we correlate the gelation temperatures and periods of stability of the gels with data from DSC, IR, optical microscopy, X-ray diffraction, and small-angle neutron scattering (SANS) to identify the factors responsible for efficient gelation. In this way, the network structures of the gels are investigated at several length scales and the gelating properties of **3**−**5** are compared with those of the corresponding alkyl perfluoroalkanoates (**6**), whose ester groups can act only as H-bond acceptors.

Experimental Section

Instrumentation. Melting point determinations (corrected) and polarized optical micrography (POM) of silicone oil gels sandwiched between thin cover slides were performed on a Leitz 585 SM-LUX-POL microscope equipped with crossed polars, a Leitz 350 heating stage, a Photometrics CCD camera interfaced to a computer, and an Omega HH503 microprocessor thermometer connected to a J-K-T thermocouple. IR spectra were obtained on a Perkin-Elmer Spectrum One FT-IR spectrometer interfaced to a PC. NMR spectra were recorded on a Varian 300 MHz spectrometer interfaced to a Sparc UNIX computer using Mercury software and were referenced to internal TMS (^{1}H), internal $CDCl_3$ (^{13}C), or trifluoroacetic acid in a sealed capillary placed in the NMR tube with the sample (^{19}F, δ −77.0 in $CDCl_3$ and

(17) (a) Shi, C.; Huang, Z.; Kilic, S.; Xu, J.; Enick, R. M.; Beckman, E. J.; Carr, A. J.; Melendez, R. E.; Hamilton, A. D. *Science* **1999**, *286*, 1540−1543. (b) Placin, F.; Desvergne, J.-P.; Cansell, F. *J. Mater. Chem.* **2000**, *10*, 2147−2149.
(18) (a) Frkanec, L.; Jokić, M.; Makarević, J.; Wolsperger, K.; Žinić, M. *J. Am. Chem. Soc.* **2002**, *124*, 9716−9717. (b) Kobayashi, H.; Friggeri, A.; Koumoto, K.; Amaike, M.; Shinkai, S. *Org. Lett.* **2002**, *4*, 1423−1426. (c) Jung, J. H.; John, G.; Masuda, M. J.; Yoshida, K.; Shinkai, S. *Langmuir* **2001**, *17*, 7229−7232.
(19) Derossi, D.; Kajiwara, K.; Osada, Y.; Yamauchi, A. *Polymer Gels: Fundamentals and Biomedical Applications*; Plenum Press: New York, 1991.
(20) Bhattacharya, S.; Ghosh, Y. K. *Chem. Commun.* **2001**, 185−186.
(21) Vidal, M. B.; Gil, M. H.; *J. Bioact. Compat. Polym.* **1999**, *14*, 243−257.
(22) Pozzo, J.-L.; Clavier, G. M.; Desvergne, J.-P. *J. Mater. Chem.* **1998**, *8*, 2575−2577.
(23) de Loos, M.; van Esch, J.; Stokroos, I.; Kellogg, R. M.; Feringa, B. L. *J. Am. Chem. Soc.* **1997**, *119*, 12675−12676.
(24) (a) Jung, J. H.; Ono, Y.; Shinkai, S. *Chem.−Eur. J.* **2000**, *6*, 4552. (b) Terech, P. *Ber. Bunsen-Ges. Phys. Chem.* **1998**, *102*, 1630−1643.
(25) (a) Kobayashi, S.; Hamasaki, N.; Suzuki, M.; Kimura, M.; Shirai, H.; Hanabusa, K. *J. Am. Chem. Soc.* **2002**, *124*, 6550−6551. (b) Jung, J. H.; Ono, Y.; Shinkai, S. *Angew. Chem., Int. Ed.* **2000**, *39*, 1862−1865. (c) Jung, J. H.; Ono, Y.; Hanabusa, K.; Shinkai, S. *J. Am. Chem. Soc.* **2000**, *122*, 5008−5009. (d) Ono, Y.; Nakashima, K.; Sano, M.; Hojo, J.; Shinkai, S. *J. Mater. Chem.* **2001**, *11*, 2412−2419.
(26) (a) LoNostro, P.; Ku, C. Y.; Chen, S. H.; Lin, J. S. *J. Phys. Chem.* **1995**, *99*, 10858−10864. (b) LoNostro, P. *Adv. Colloid Interface Sci.* **1995**, *56*, 245−287.
(27) Höpken, J. Proefschrift. Ph.D. Thesis, University of Twente, The Netherlands, 1991.
(28) (a) Twieg, R. J.; Russell, T. P.; Siemens, R.; Rabolt, J. F. *Macromolecules* **1985**, *18*, 1361−1362. (b) Rabolt, J. F.; Russell, T. P.; Siemens, R.; Twieg, R. J.; Farmer, B. *Polym. Prepr. (Am. Chem. Soc., Div. Polym. Chem.)* **1986**, *27*, 223−224. (c) Pugh, C.; Höpken, J.; Möller, M. *Polym. Prepr. (Am. Chem. Soc., Div. Polym. Chem.)* **1988**, *29*, 460−461.
(29) Ku, C.-Y.; LoNostro, P.; Chen, S.-H. *J. Phys. Chem. B* **1997**, *101*, 908−914.
(30) Terech, P.; Rodriguez, V.; Barnes, J. D.; McKenna, G. B. *Langmuir* **1994**, *10*, 3406−3418.
(31) Höpken, J.; Pugh, C.; Richtering, W.; Möller, M. *Makromol. Chem.* **1988**, *189*, 911−925.
(32) Krafft, M.-P.; Riess, J. G. *Angew. Chem., Int. Ed. Engl.* **1994**, *33*, 1100−1101.
(33) (a) Loiseau, J.; Lescanne, M.; Colin, A.; Fages, F.; Verlhac, J.-B.; Vincent, J.-M. *Tetrahedron* **2002**, *58*, 4049−4052. (b) Emmanouli, V.; Choul, M. E.; André-Barrès, C.; Guidetti, B.; Rico-Lattes, I.; Lattes, A. *Langmuir* **1998**, *14*, 5389−5395.
(34) Challis, B. C.; Challis, J. A. In *Comprehensive Organic Chemistry*; *The Synthesis and Reactions of Organic Compounds*; Barton, D. H. R.; Ollis, W. D., Eds.; Pergamon Press: New York, 1979; Vol. 2, p 957.
(35) (a) Jokić, M.; Makarević, J.; Žinić, M. *J. Chem. Soc., Chem. Commun.* **1995**, 1723−1724. (b) Makarević, J.; Jokić, M.; Perić, B.; Tomišić, V.; Kojić-Prodić, B.; Žinić, M. *Chem.−Eur. J.* **2001**, *7*, 3328−3341. (c) Luo, X.; Liu, B.; Liang, Y. *Chem. Commun.* **2001**, 1556−1557. (d) Suzuki, M.; Yumoto, M.; Kimura, M.; Shirai, H.; Hanabusa, K. *Chem. Commun.* **2002**, 884−885. (e) Makarević, J.; Jokić, M.; Frkanec, L.; Katalenić, D.; Žinić, M. *Chem. Commun.* **2002**, 2238−2239. (f) Suzuki, M.; Yumoto, M.; Kimura, M.; Shirai, H.; Hanabusa, K. *Chem.−Eur. J.* **2003**, *9*, 348−354.

Table 1. Appearances,[a] T_g Values (°C in parentheses), and Periods of Stability[b] of Gels Containing 2 wt % **1**, **3a**−**c**, **5**, and **6a**,**b** in Various Liquids

liquid	1b	3a	3b	3c	5	6a	6b
hexane	P	S	S	TG (35−38)[d]	CG (20−25)[h,i]	S	S
n-octane	P	S	S	TG (47−51)[e]	P	S	S
silicone oil	P	P	P	TG (70)[c]	OG (98)[h]	S	TG (50−54)[j]
ethanol	P	S	P	TG (60)[f]	CG (78)[h,i]	S	S
1-butanol	P	S	P	TG (33−36)[d]	CG (93)[h]	S	S
1-octanol	P	P	P	TG (8−15)[d]	TG (85)[h]	S	TG (18−20)[j]
benzyl alcohol	P	S	S	TG (61−63)[c]	OG (>98)[h]	S	S
DMSO	TG (45)[c]	P	P	P	P	P	TG (42−49)[j]
toluene	P	S	S	TG (38−40)[g]	OG (25−30)[h]	S	S
CCl_4	P	S	S	TG (<5)[d]	P	S	S
n-perfluorooctane	P	S (13)	P	OG (75−80)[h]	TG (83)[h,i]	S	OG (40)[h]

[a] S-solution; P-precipitate; CG-clear, transparent gel; TG-turbid gel; OG-opaque gel. [b] In sealed tubes at 25 °C. [c] Stable for >15 months. [d] Stable for <1 week. [e] Stable for 2 months. [f] Stable for 6 weeks. [g] Stable for 1 month. [h] Stable for >4 months. [i] Slow cooling in air. [j] Stable for >13 months.

−76.9 in acetone-d_6). Unless stated otherwise, elemental analyses were performed on a Perkin-Elmer 2400 CHN elemental analyzer. Differential scanning calorimetry (DSC) was performed on a TA 2910 differential scanning calorimeter interfaced to a TA Thermal Analyst 3100 controller. All DSC data are reported at temperatures of maximum heat flow. Heating rates were 5 °C/min; cooling rates were variable and depended on the difference between the cellblock and ambient temperatures. X-ray diffraction (XRD) of samples in thin, sealed capillaries (0.5 mm diam; W. Müller, Schönwalde, FRG) was performed on a Rigaku R-AXIS image plate system with Cu Kα X-rays (λ = 1.54056 Å) generated with a Rigaku generator operating at 46 kV and 46 mA. Data processing and analyses were performed using Materials Data JADE (version 5.0.35) XRD pattern-processing software.[36] Molecular calculations of lowest-energy conformations and molecular dimensions were performed with the semiempirical Parametric Method 3 (PM3)[37] of the HYPERCHEM package, release 5.1 Pro for Windows from Hypercube, Inc.

SANS experiments over the q range from 0.0009 to 0.235 Å^{-1} were carried out using the 30 m SANS instruments at the National Center for Neutron Research of the National Institute of Standards and Technology.[38] Gels for SANS investigations were prepared with benzene-d_6 or 1-butanol-d_{10} as the liquid in 2 mm quartz cells. The scattered intensity was corrected for background and parasitic scattering,[39] placed on an absolute level using a direct measurement of the beam flux, and circularly averaged to yield the scattered intensity, $I(q)$, as a function of the wave vector, q, where $q = (4\pi/\lambda)\sin(\theta/2)$ (λ is the wavelength of the neutrons, and θ is the scattering angle). A given level of flat incoherent background due to the intrinsic protons of the gelators has been subtracted from the reduced SANS data. This level had a weak amplitude and affected noticeably only the large angle part of the scattering curves. The related amplitude of this correction was made by assuming that the large q asymptotic behavior is strictly a q^{-4} intensity decay. The densities of both **3c** and **4d** were taken to be 1.4 g/cm^3. The volume contrasts are -4.26×10^{10} cm^{-2} in benzene-d_6 and -4.88×10^{10} cm^{-2} in 1-butanol-d_{10} (**3c**) and -3.51×10^{10} cm^{-2} in benzene-d_6 and -4.61×10^{10} cm^{-2} in 1-butanol-d_{10} (**4d**).

Materials. Silicone oil (tetramethyltetraphenylsiloxane; Dow silicone oil 704) was used as received. Other liquids (Aldrich) for the preparation of gels were reagent grade or better. Oxalyl chloride (99%), ethylamine (2.0 M solution in tetrahydrofuran), 1-propylamine (99%), 1-butylamine (99.5%), 1-amylamine (99%), 1-hexylamine (99%), 1-octylamine (99%), 1-decylamine (95%), and pentadecafluorooctanoyl chloride (97%) were from Aldrich and were used as received. 1-Octadecylamine (Aldrich) was distilled twice at 160−165 °C at 1 torr and stored under a nitrogen atmosphere. Perfluorododecanoic acid (96%) and perfluorooctadecanoic acid (95%) from Fluorochem were used as received.

General Procedure for the Synthesis of Perfluoroacid Derivatives. Syntheses of esters and amides of the perfluoroalkanoic acids are outlined in Scheme 1. For instance, perfluorododecanoyl chloride was prepared by adding oxalyl chloride (3 mL, 0.034 mol) slowly to a stirred solution of the perflourododecanoic acid (5.00 g, 0.00814 mol) in dry benzene (25 mL) under a nitrogen atmosphere. The temperature was raised to ca. 60 °C, and stirring was continued under a nitrogen atmosphere for 12 h. Excess oxalyl chloride and solvent were then removed by distillation under reduced pressure, and the residue was used directly in the subsequent estification/amidation step.[40]

Under a nitrogen atmosphere, a few drops of pyridine were added to a stirred mixture of an acid chloride (1 equiv) and an amine or alcohol (1 equiv) in dry benzene. After 5 min, the temperature was raised to ca. 60 °C, and stirring was continued under nitrogen for 12 h. The reaction mixture was then added to dilute hydrochloric acid (5%) and extracted with 1:1 ethyl acetate/hexane. Evaporation of the organic extracts yielded the crude product. It was purified further by sublimation under vacuum (ca. 1 torr). Spectroscopic and analytical data for **3**−**6** are collected in Supporting Tables 1−3.

Preparation of Gels and Determination of Gelation Temperatures. Weighed amounts of a liquid and a solid were placed into a glass tube (5 mm i.d.) that was usually flame-sealed (to avoid evaporation). The tubes were heated twice in a water bath (until all solid material dissolved) to ensure homogeneity and cooled rapidly by being plunged in an ice−water mixture. In cases where this cooling protocol did not lead to gels, the hot samples were allowed to cool more slowly in the air at ambient temperatures and gelation was assessed at room temperature. Gelation temperatures (T_g) were determined by the inverse flow method.[41] A gel in a sealed glass tube was inverted, strapped to a thermometer near the bulb, and immersed in a stirred water bath at room temperature. The temperature of the bath was raised slowly, and the range of T_g was taken from the point at which the first part of the gel was observed to fall to the point at which all had fallen under the influence of gravity. Gel samples for SANS analyses were prepared in closed quartz cells (2 mm i.d.) in benzene-d_6 (99.5% D) or 1-butanol-d_{10} (98% D) (Cambridge Isotope Laboratories) under an inert atmosphere.

Results and Discussion

Gelation Studies. Several general observations can be made from the data collected in Tables 1 and 2 for gelation studies of 2 wt % **1b** and **3**−**6**. For instance, DMSO is the only liquid

(36) *Jade*, version 5.0.35 (SPS); 2000 release; Materials Data Inc.: Livermore, CA.
(37) Stewart, J. J. P. *J. Comput. Chem.* **1989**, *10*, 209−220.
(38) Glinka, C. J.; Barker, J. G.; Hammouda, B.; Krueger, S.; Moyer, J. J.; Orts, W. J. *J. Appl. Crystallogr.* **1998**, *31*, 430−445.
(39) *NG3 and NG7 30-Meter SANS Instruments Data Acquisition Manual.* Cold Neutron Research Facility at the National Institute of Standards and Technology: Gaithersburg, MD, 2002.
(40) The primary amide **4a** was prepared by bubbling ammonia (generated by heating aqueous ammonium hydroxide and passing the gas through a $CaSO_4$ drying tube) through a chloroform solution of **2b**. The precipitate that formed was filtered, dried under house vacuum, and sublimed.
(41) Takahashi, A.; Sakai, M.; Kato, T. *Polym. J.* **1980**, *12*, 335−341.

Table 2. Appearances,[a] T_g Values (°C in parentheses), and Periods of Stability[b] of Gels Containing 2 wt % **4a**−**g** in Various Liquids

liquid	4a	4b	4c	4d	4e	4f	4g
hexane	P	P	TG (49)[e]	CG (48)[h]	CG (44)[i]	CG (35−38)[j]	P
n-octane	P	P	CG (66)[f]	CG (60)[h]	CG (58)[i]	P	P
silicone oil	OG (>98)[c]	TG (48−50)[d]	TG (86)[f]	TG (98)[h]	TG (102)[i]	TG (96)[k]	TG (24)[d]
ethanol	P	CG (18)[d]	CG (39)[f]	CG (41)[h]	CG (37)[i]	CG (42)[k]	P
1-butanol	jelly	CG (∼0)[d]	CG (38)[f]	CG (39)[h]	CG (28−29)[i]	CG (32)[k]	P
1-octanol	TG (63−67)[c]	TG (27)[d]	TG (52)[f]	CG (49−53)[h]	CG (34−47)[i]	TG (39)[k]	P
benzyl alcohol	jelly	P	TG (65)[f]	TG (90−93)[h]	TG (91)[i]	TG (89)[k]	TG (50)[d]
DMSO	P	TG (26)[d]	TG (63)[f]	TG (68)[h]	TG (64)[i]	TG (65)[k]	TG (26)[d]
toluene	P	TG (51)[d]	TG (56)[f]	TG (48)[h]	TG (47)[i]	TG (48)[k]	P
CCl_4	P	P	TG (54)[f]	TG (56)[h]	TG (51)[i]	TG (46−48)[k]	P
n-perfluorooctane	P		TG (57)[g]	TG (58)[c]	TG (60)[c]		

[a] P-precipitate; CG-transparent gel; TG-turbid gel. [b] In sealed tubes at 25 °C. [c] Stable for 3 months. [d] Stable for <3 weeks. [e] Stable for >20 months, (syneresis after 5 months). [f] Stable for >20 months. [g] Stable for >4 months. [h] Stable for >14 months. [i] Stable for >12 months. [j] Stable for >16 months (syneresis after 2 months). [k] Stable for >16 months. [l] Stable for >22 months. [m] Stable for >22 months (syneresis after 2 months).

that forms a gel stable at room temperature with **1b**. Among the LMOGs derived from the shorter perfluoro acid **1a**, only **3c** gelates several liquids. Although **6a** (the ester corresponding to the very good LMOG, **4c**) was soluble in all liquids examined (except DMSO), the longer ester **6b** gelates four of the eleven liquids examined and the gels have long periods of stability. Compound **5**, with its longer perfluoroalkyl chain, underwent macroscopic phase separation in hot solutions of hexane, ethanol, or *n*-perfluorooctane when they were cooled rapidly (by dipping their containers in an ice−water mixture), but stable gels were formed when these solutions were cooled more slowly (in air). In all other cases when the fast gelation protocol was unsuccessful, the slow cooling one was attempted, and it was unsuccessful as well. Only in the case of gelation by **5** does there appear to be a discernible rate of cooling dependence on the nucleation growth of the fibrillar networks from the hot, supersaturated (sol) phases. We have not attempted other cooling protocols, nor have we examined in depth the dependence of **5**.

Although elongation of the perfluoroalkyl chain length from seven (**3a**) to eleven (**4c**) carbon atoms enhances gelation ability, further elongation to 17 perfluoromethylene units (**5**) does not. However, gels of 2 wt % **5** whose T_g values are significantly higher than those of **4c** were observed in alcohols, silicone oil, and *n*-perfluorooctane. These results suggest that intermolecular H bonding between amide groups is important to gelator aggregation, and the presence of such bonding is evidenced by infrared spectroscopic studies (vide infra).

In addition, the involvement of London dispersion forces in stabilizing the aggregates is suggested by the generally superior gelating properties (as assessed by the types of liquids gelated and the temporal and thermal gel stabilities) of the LMOGs with longer alkyl chains. However, the gelation abilities of **4** increase with increasing alkyl chain length from two to four carbon atoms (**4d**) and then decrease. At 2 wt %, **4c**−**e** gelated all the liquids examined. The variation of T_g for silicone oil and DMSO gels with 2 wt % of the homologues **4b**−**g** are shown graphically in Figure 1. The primary amide **4a** ($n = 0$) has additional possible H-bonding interactions that are indicated by the anomalously high T_g (>98 °C) of its 2 wt % silicone oil gel.

Concentration-dependent studies of silicone oil gels with **4d**, the most efficient LMOG, have been conducted (Figure 2 and Supporting Table 4). A jelly is formed at 0.1 wt % and gels form at 0.2 wt % and larger concentrations; the gels with ≥0.3 wt % have been stable for more than 11 months at room temperature in sealed vials! T_g increases rapidly with concentration of **4d** to ca. 2.0 wt % and then is virtually independent of concentration to 5 wt %. In the lower concentration range, fibril interactions and other associations related to the gelator network are not complete.[15]

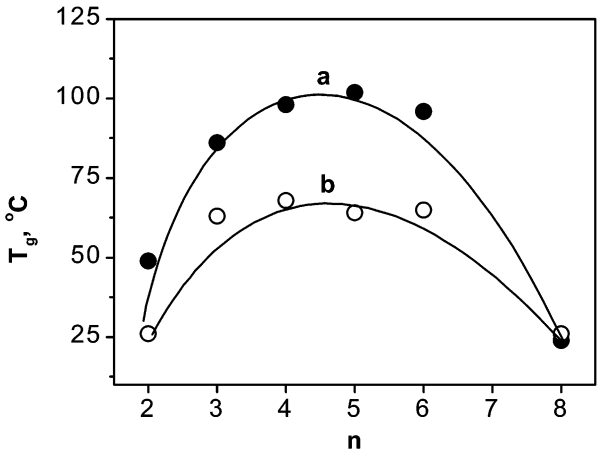

Figure 1. T_g values (°C) of 2 wt % **4b**−**g** versus *n*, the number of carbon atoms in the aliphatic chain in (a, ●) silicone oil and (b, ○) DMSO. The curves have no physical significance; they are included as a visual guide.

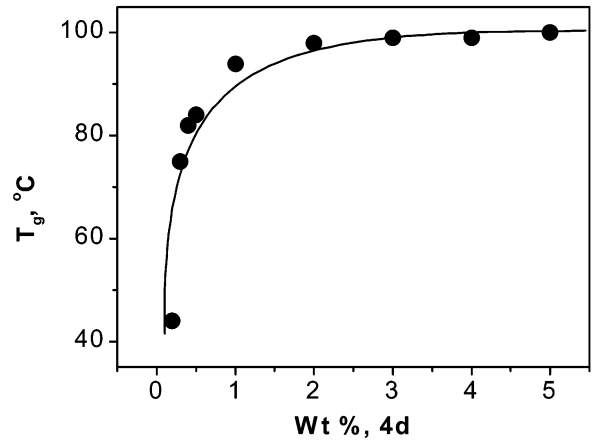

Figure 2. T_g versus concentration of **4d** in silicone oil gels (all are turbid in appearance). The curve has no physical significance; it is included as a visual guide.

Relatively low concentrations of some of the LMOGs described here are able to gelate a *perfluorinated n*-alkane liquid, *n*-perfluorooctane, as well. For instance, as little as 0.25 wt % of **4c** gelates *n*-perfluorooctane, and the gels with 0.25 to 5 wt % of **4c** have been stable at room temperature in sealed vials for more than 4 months (Supporting Table 5). Unlike the T_g

Table 3. Melting Temperatures (°C) and Heats of Transition (J/g; in parentheses) of Neat **3**−**6** by Polarizing Optical Microscopy (POM) and Differential Scanning Calorimetry (DSC)

		DSC		
LMOG	POM	1st cycle	2nd cycle	3rd cycle
3a	37.6−37.8	34.4 (30.0)[a]	35.9 (32.9)[a]	35.9 (31.9)[a]
		31.4 (−22.4)[b]	32.8 (−22.9)[b]	31.0 (−33.7)[b]
3b	70.3−70.7	65.7 (186.9)[a]	65.5 (156.8)[a]	–
		58.0 (−114.0)[b]	57.6 (−108.5)[b]	
3c	91.7−92.0	88.4 (129.6)[a]	88.1 (130.3)[a]	88.1 (127.1)[a]
		79.3 (−130.8)[b]	79.0 (−129.7)[b]	78.9 (−129.0)[b]
4a	178.6−179.9	172.9 (66.1)[a,c]	–	–
4b	110.6−111.0	110.3 (103.6)[a]	110.2 (91.1)[a]	110.2 (83.4)[a]
		103.1 (−90.4)[b]	102.5 (−39.3)[b,d]	102.9 (−53.0)[b,d]
			101.0 (−29.4)[b]	100.1 (−1.7)[b]
4c	105.9−106.8	102.3 (89.6)[a]	102.1 (15.5)[a]	–
		93.1 (−15.7)[b]	93.2 (−5.9)[b]	
4d	94.8−95.0	99.4 (45.8)[a]	99.2 (41.3)[a]	–
		94.8 (−40.6)[b]	94.7 (−38.8)[b]	
4e	93.6−94.5	99.7 (45.5)[a]	99.7 (42.6)[a]	–
		94.7 (−40.5)[b]	94.9 (−40.5)[b]	
4f	96.5−97.1	98.7 (101.5)[a]	98.6 (89.0)[a]	98.3 (72.1)[a]
		92.4 (−82.5)[b]	92.2 (−70.9)[b]	91.5 (−57.3)[b]
4g	101.2−101.5	73.4 (53.8)[a,d]	100.7 (84.2)[a]	100.7 (83.7)[a]
		82.1 (3.1)[a,d]	93.9 (−76.8)[b]	94.0 (−77.9)[b]
		97.9 (64.73)[a,d]		
		100.3 (37.4)[a]		
		93.70 (−79.2)[b]		
5	164.7−165.8	158.7 (58.4)[a]	159.7 (55.2)[a]	159.7 (50.0)[a]
		154.2 (−38.7)[b]	154.3 (−35.8)[b]	154.2 (−31.7)[b]
		123.0 (−9.1)[b,d]	123.3 (−8.1)[b,d]	122.9 (−7.4)[b,d]
6b	54.9−55.6	54.4 (17.2)[a,c]	54.4 (45.5)[a,d]	–
		56.2 (84.6)[a]	56.0 (53.3)[a]	
		51.8 (−58.1)[b,d]	51.6 (−53.4)[b,d]	
		51.3 (−42.2)[b]	51.0 (−42.9)[b]	

[a] Heating. [b] Cooling. [c] Sublimed partially during melting; heats are inaccurate. [d] Solid−solid-phase transition.

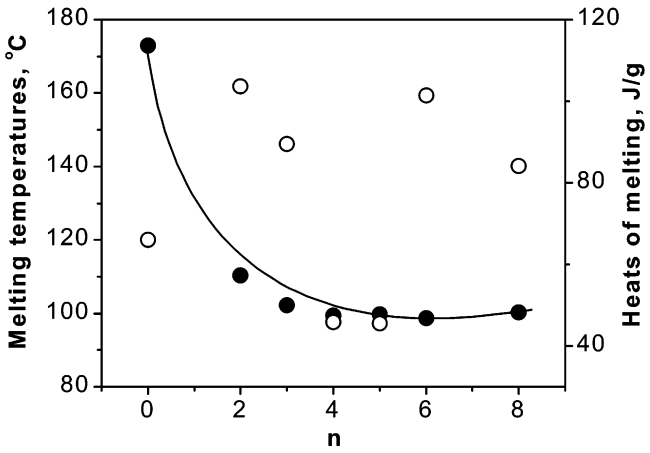

Figure 3. Melting temperatures (●) and heats of melting (○; first heating) of neat **4** homologues as a function of the number of carbon atoms (n) in the *N*-alkyl chain segments. The curve has no physical significance; it is included as a visual guide to the trends.

values of the silicone oil gels (Figure 2), those of the *n*-perfluorooctane gels continue to increase between 0.5 and 5 wt % of **4c** (Supporting Figure 1).

Thermal Properties. The melting temperatures of the perfluoroalkyl amides vary with the length of both the alkyl and perfluoroalkyl segments (Table 3). As the aliphatic chain lengths of **4a**−**g** increase, their melting temperatures decrease (as do the gelating abilities of the LMOGs) and then slowly increase (Figure 3). In addition, ΔH_{fus} of the homologues with 3−5 carbon atoms (**4c**−**e**) in their alkyl chains is much lower than

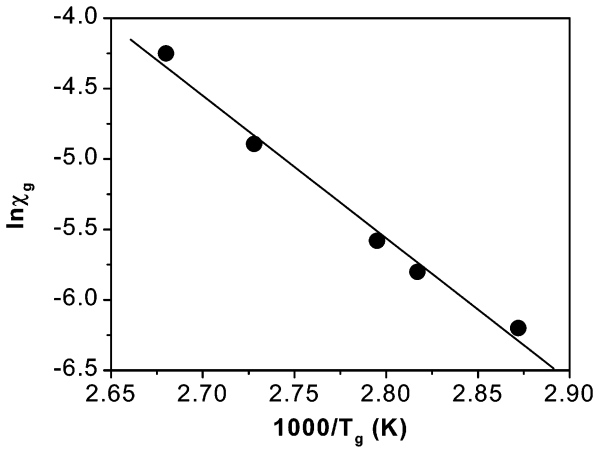

Figure 4. Semilog plot of the mole fraction of **4d** in silicone oil (χ_g) versus the inverse of gelation temperature (T_g).

that of the other shorter and longer homologues; perhaps not coincidentally, **4c**−**e** are the only LMOGs that gelated all of the liquids investigated.

The slope and intercept of the best linear fit to the data in Figure 4 for silicone oil gels of **4d** have been interpreted according to the Schröder−van Laar equation (eq 1),[42] assuming that the gels form ideal solutions on heating. This assumption is not totally correct for several reasons, including the fact that sols form above T_g. Nevertheless, the calculations provide useful insights. In eq 1, ΔH_{fus} and T_{fus} are the enthalpy of melting of the gel assemblies and the melting temperature of the neat gelator, respectively.

$$\ln X_g = \frac{\Delta H_{fus}}{RT_g} + \frac{\Delta H_{fus}}{RT_{fus}} \quad (1)$$

The isomorphous nature of the packing arrangements of the neat solids and gel networks of **4d** (vide infra) allows direct comparisons between the values of ΔH from DSC heating thermograms of the neat solids and ΔH_{fus}. We hypothesize that the nearer the two values, the smaller the influence of the liquid component on the dissolution of the gelator network at T_g. Since the values of ΔH_{fus} of **4d** (89 J/g) are somewhat less than the ΔH values calculated from Figure 4 (117 J/g from the slope and 97 J/g from the intercept), solvent−gelator interactions appear to *stabilize* the gel network.

IR Spectral Studies. IR peaks characteristic of the carbonyl and amino moieties appear at similar spectral positions in neat powders of the amide LMOGs and in their gels (Table 4 and, for example, Figure 5). The N−H and C═O frequencies are much lower than expected for free groups and fall within the expected ranges of H-bonded ones.[43]

Polarizing Optical Microscopy (POM). The aggregates of **4c**−**f** and **5** in silicone oil were not observable by our microscope. Optical micrographs of gels containing 2 wt % **3c**, **4b**, or **6b** in silicone oil show elongated and strand-like aggregates (parts a, b, and d of Figure 6). Although individual stands are difficult to discern within bundles at these magnifications, strand lengths are clearly in the 10−100 μm range. Even

(42) (a) Atkins, P. W. *Physical Chemistry*, 5th ed.; Freeman: New York, 1994; p 227. (b) Moore, W. J. *Physical Chemistry*, 4th ed.; Prentice Hall: Englewood Cliffs, NJ, 1972; p 249.
(43) Rao, C. N. R. *Chemical Applications of Infrared Spectroscopy*; Academic Press: New York, 1963; pp 258−263.

Table 4. Characteristic IR Frequencies (cm^{-1}) of Neat **3** and **4** and Their 2 wt % Gels in Silicone Oil

	neat powder		gel	
LMOG	ν_{N-H}	$\nu_{C=O}$	ν_{N-H}	$\nu_{C=O}$
3a	3323	1693	*a*	*a*
3b	3336	1691	*a*	*a*
3c	3345	1690	3345	1689
4b	3310	1698	3310	1697
4c	3324	1694	3323	1695
4d	3325	1694	3330	1695
4e	3325	1692	3324	1693
4f	3324	1692	3329	1694
4g	3346	1689	3349 (5 wt %)	1690 (5 wt %)

[a] No gelation.

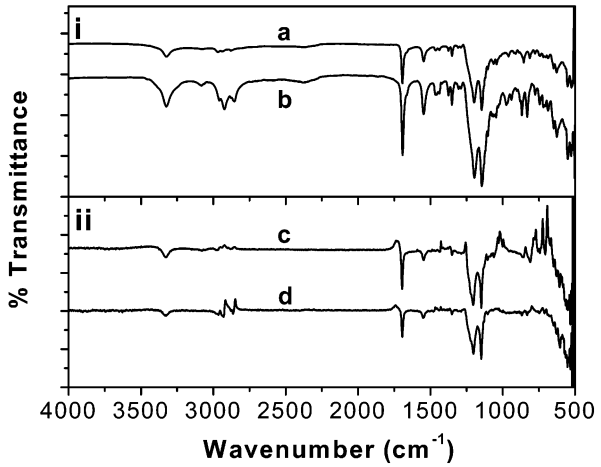

Figure 5. IR spectra of (a) neat **4c**, (c) its 2 wt % gel in silicone oil, (b) neat **4e**, and (d) its 2 wt % gel in tetradecane. In (c) and (d), the contributions from the liquids have been subtracted approximately.

though rather long fibers are seen in the gel of **4b** in silicone oil and the melting temperature of the neat LMOG is very high (ca. 110 °C), its thermal (T_g = 48−50 °C) and temporal (<1 week) stabilities are lower than those of the other gelators in the same series in all liquids examined (Table 2). Shorter aggregates are observed for 2 wt % silicone oil gels of **4g** (Figure 6c), consistent with its low thermal (T_g = 24 °C) and short temporal stabilities (<3 weeks).

X-ray Diffraction Studies. The X-ray diffraction peaks of the assemblies of gels containing 2 wt % **3**−**6** in silicone oil were obtained by subtracting the "amorphous scatter" of the liquid components from the total gel diffractograms (Figures 7−9 and Supporting Figures 2−6)[44,45] and are compared with diffraction patterns of the neat powders. The POM of each of the gels (not all shown) provides no evidence for nonfibrillar LMOG crystallites. This supports our contention that the diffraction patterns are from the gelator networks.

Although some peaks from the gels are weak, they generally coincide with peaks from the neat powders. Diffractograms of each LMOG as neat powders and in gels possess a low-angle peak from which the layer thickness (*d*) has been calculated using Bragg's law (Table 5). The higher-order reflections of the low-angle peak are consistent with a 1/2, 1/3, 1/4, etc. distance relationship as expected of a layered, fibrillar assembly. A similar packing has been proposed for gelator networks of the diblock molecule, heptadecafluorotetracosane.[29a] For each of our compounds, including **3c,** the *d* values of the neat solid and gel are similar. When the aliphatic chain contains eight or more carbon atoms, the *d* value is approximately 1.5 times the calculated extended length of the molecule.[46] Partial interdigitation of (nearly) extended molecules in orthogonally packed layers (Figure 10a) and tilted, extended molecules within noninterdigitated layers (Figure 10c; tilt angles calculated in Table 5) are two possible arrangements. When the aliphatic chains contain less than eight carbon atoms, the *d* values are slightly smaller than the calculated molecular length and the molecules may be fully interdigitated as indicated in Figure 10b. Although not shown in Figure 10, the H bonding evident in the IR spectra (Table 4) must be important in aligning neighboring molecules, and each of the packing arrangements allows for it.

SANS Studies. The SANS technique uses the Fourier transform of large-scale neutron-scattering length density fluctuations[47,48] in a system. SANS is able to characterize the structures of nanoparticles in a dispersing medium, and in particular, self-assembled networks in molecular gels.[49] Brief analyses of the scattering curves from gels with two of the LMOGs in Scheme 1, **3c** and **4d**, with benzene-d_6 or 1-butanol-d_{10} are included here. More detailed analyses will be provided elsewhere.[50]

Gels with 4d as LMOG. Figure 11 shows the radially averaged, 2-dimensional experimental scattering curves of the **4d** gels in benzene-d_6 and 1-butanol-d_{10}. Clearly, self-aggregation of **4d** is extremely sensitive to both the liquid type and the concentration of the gelator (in benzene-d_6).

In butanol-d_{10}, the scattering curves show a Q^{-1} power law decay followed by a sharper one (Q^{-4}) on which is superimposed a first well-defined oscillation at larger angles (Q = 0.0327 Å^{-1}) and a second one at Q = 0.073 Å^{-1}. These scattering features are characteristic of a form-factor intensity corresponding to unidimensional scatterers (i.e., with rather monodisperse cross-sections) as described by eq 2. The scattering profile can be fitted satisfactorily[49,51] to a theoretical curve for randomly distributed cylindrical fibers (r_0 = 165 Å). In eq 2, M_L is the molecular weight of the fiber per unit length, r_0 is its geometrical radius, J_1 is the Bessel function of the first kind, and Δb^2_{spec} is the specific contrast of the fiber in a given solvent. C, the gelator concentration involved in the fibers, is expressed in g cm^{-3}.

$$I(Q) = \pi C M_L \Delta b^2_{spec} [2J_1(Q_r)/Q_r]^2 \qquad (2)$$

In benzene-d_6, the situation appears more complex. Curves show a power law decay ($Q^{-1.6}$ for 2 wt % and $Q^{-1.7}$ for 1 wt %) followed by a Q^{-4} decrease on which is superimposed a first oscillation at $Q \approx 0.027$ Å^{-1} and a more poorly resolved one at $Q \approx 0.08$ Å^{-1}. These scattering features are typical of

(44) Ostuni, E.; Kamaras, P.; Weiss, R. G. *Angew. Chem., Int. Ed. Engl.* **1996**, *35*, 1324−1326.
(45) X-ray diffraction patterns of **3a** and **3b**, both nongelators for the liquids examined, are shown in Supporting Figure 7.
(46) Calculated by Hyperchem (version 5.1) molecular modeling system at the PM3 level, adding the van der Waals radii[46a] of the terminal atoms. (a) *Lange's Handbook of Chemistry*; 13th ed.; Dean, A. J., Ed.; McGraw-Hill: New York, 1985; Sect. 3, pp 121−126.
(47) Guinier, A.; Fournet, G. *Small Angle Scattering of X-rays*; Wiley: New York, 1955.
(48) Glatter, O.; Kratky, O. *Small-Angle X-ray Scattering*; Academic Press: London, 1982.
(49) Terech, P.; Volino, F.; Ramasseul, R. *J. Phys. (Paris)* **1985**, *46*, 895−903.
(50) George, M.; Snyder, S. L.; Glinka, C. J.; Terech, P.; Weiss, R. G., to be submitted for publication.
(51) Vainshtein, B. K. *Diffraction of X-rays by chain molecules*, Elsevier: Amsterdam, 1966.

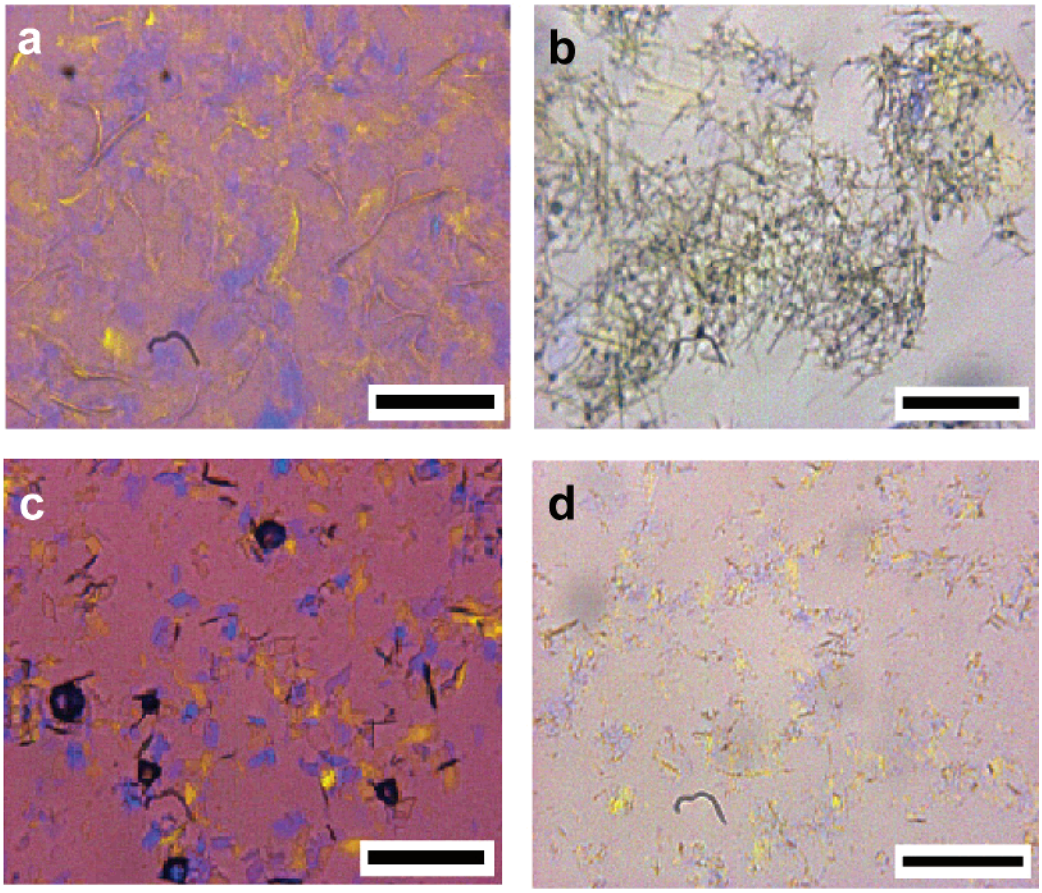

Figure 6. Polarizing optical micrographs (room temperature) of 2 wt % (a) **3c**, (b) **4b**, (c) **4g**, and (d) **6b** gels in silicone oil. Black space bars are 100 μm. The images were taken with a full-wave plate.

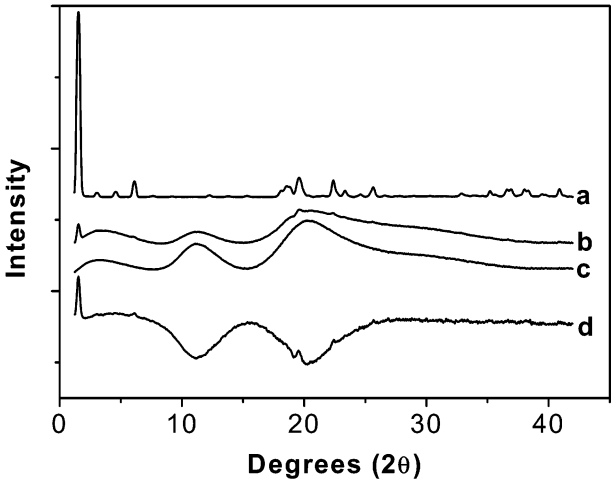

Figure 7. X-ray diffraction patterns (room temperature) of **3c**: (a) powder, (b) 2 wt % gel in silicone oil, (c) neat silicone oil, and (d) diffractogram (b) − diffractogram (c) and magnified 5 times.

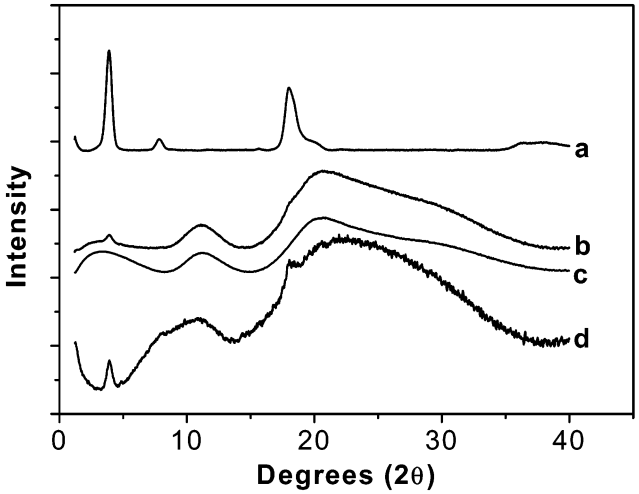

Figure 8. X-ray diffraction patterns (room temperature) of **4d**: (a) powder, (b) 2 wt % gel in silicone oil, (c) neat silicone oil, and (d) diffractogram (b) − diffractogram (c) and magnified 4 times.

fiberlike aggregates involved in a network with different hierarchical aggregation modes. The relative departure from the expected low-Q Q^{-1} behavior for long, rigid cylinders and its variation with concentration confirm that interferences between fibers participate in the scattering. In such LMOG networks, attractions between fibers can produce thicker aggregates or bundles acting as junction zones. Among the different situations available for such interactions, merged and/or entwined fibers are frequently observed.[52] Despite the gels being dilute systems (gelator concentrations ≤4 wt %), additional contributions from (i) the junction zones, (ii) other types of aggregates (e.g., short rods), and (iii) interfiber interferences can complicate the scattering. Attempts to separate the inter- and intraparticle correlations will be made in a more detailed analysis.[50]

A clear Q^{-1} low-Q decay and a pronounced first oscillation can be observed in Figure 11. The scattering profile can be fitted

(52) Terech, P.; Wade, R. H. *J. Colloid Interface Sci.* **1988**, *1252*, 542−551.

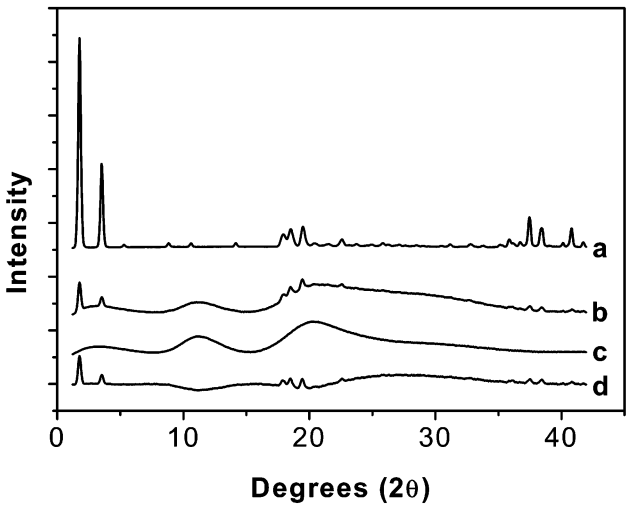

Figure 9. X-ray diffraction patterns (room temperature) of **4g**: (a) powder, (b) 2 wt % gel in silicone oil, (c) neat silicone oil, and (d) diffractogram (b) − diffractogram (c).

Table 5. Lamellar Spacings (*d*, Å) and Potential Tilt Angles (deg; see Figure 10c and text) from the Lowest-Angle Peaks in X-ray Diffraction Patterns of Neat Powders, Gels in Silicone Oil, and Calculated Extended Molecular Lengths (Å) for Compounds **3**−**6**

	extended	powder		gel (silicone oil)	
LMOG	molecular length	*d*	tilt angle	*d*	tilt angle
3a	18.6	16.0		no gelation	−
3b[a]	26.4	42.6	36	47.2	27
3c[a]	36.5	57.7	38	57.7	38
4a[b]	19.5	17.3		*c*	
4b[b]	22.7	19.8		19.8	
4c[b]	23.9	21.4		21.5	
4d[b]	25.2	22.6		22.3	
4e[b]	26.4	23.6		23.6	
4f[b]	27.7	24.8		24.8	
4g[b]	30.2	50.0	34	50.0	34
5[b]	32.1	28.8		30.1	
6b[a]	42.7	67.6	38	66.7	39

[a] 5 wt %. [b] 2 wt %. [c] No detectable peak.

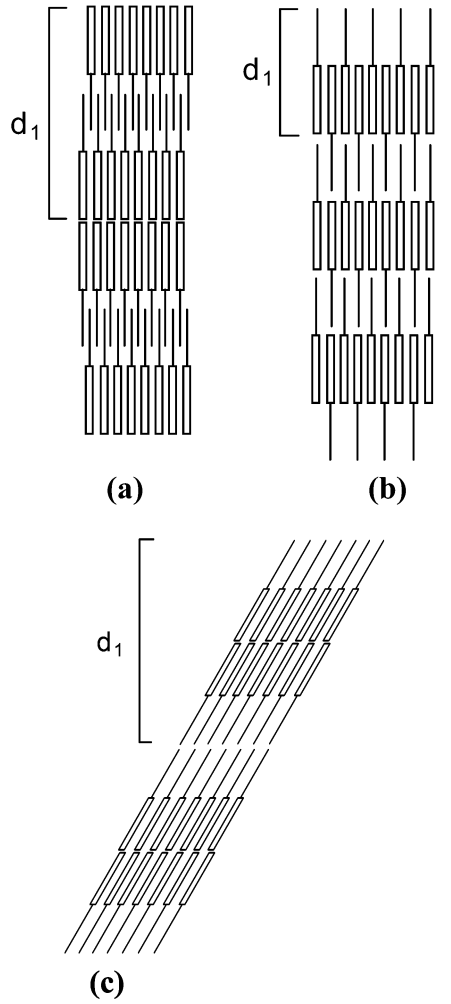

Figure 10. Three possible packing arrangements for the *N*-alkyl perfluoroalkanamides in gel aggregates and distances *d* corresponding to the low-angle X-ray diffraction peaks. The lines and rectangles represent alkyl and perfluoroalkyl segments, respectively.

satisfactorily to a theoretical curve for randomly distributed cylindrical fibers (eq 2), with radii of ca. 165 Å.

The scattering curves of the **4d** gels in 1-butanol-d_{10} are simpler than those in benzene-d_6. It is reasonable to assume that the distance $d = 165$ Å is also a representative correlation distance in the morphology of **4d** aggregates in benzene. Differences between the mechanisms of gelator fiber interactions in 1-butanol and benzene gels are revealed by the corresponding SANS signals.

Gels with 3c as LMOG. Figure 12 shows a typical intensity versus Q scattering curve for a **3c** gel in 1-butanol-d_{10}. The profile is a monotonic and sharp Q^{-4} intensity decay followed by an intense Bragg peak at $Q = 0.105$ Å^{-1}. A similar curve is observed for gels of **3c** in benzene (not shown). By contrast with **4d** organogels, no concentration or solvent dependence has been observed with **3c** gels. The SANS signatures of **3c** organogels characterize networks made up of much thicker aggregates than those of **4d** gels. Future work will attempt to quantify the typical correlation lengths in this system.[50]

Within these large aggregates, the **3c** molecules are periodically packed in planes separated by ca. 59 Å. This distance is in excellent agreement with the 57.7 Å found in the neat powder and silicone oil gel of **3c** by X-ray diffraction (Table 5). These large dimensions can be found in the fibers themselves or in bundles of fibers acting as nodal junctions in the network. Regardless, the networks of the **3c** gels have a more pronounced crystalline character than those of the **4d** organogels.

Conclusions

We have demonstrated that *N*-alkyl perfluoroalkanamides and, to a lesser extent, esters, are efficient gelators of a variety of organic liquids, including some that have been difficult to gelate historically; both are more efficient LMOGs than underivatized diblock perfluoroalkylalkanes.[27−29,31] The incompatibility of the alkyl and perfluoroalkyl units produces supramolecular aggregates that are stabilized further by H bonding among amide groups (and, perhaps, to a lesser extent, by dipolar interactions between carboxyl groups).[53] We attribute the general sequence of gelating abilities—amides > esters > alkanes—to the presence or absence of the intermolecular interactions discussed above because all three types of LMOGs develop fibrillar assemblies in which the molecules are packed in layers.

(53) We have obtained additional evidence recently for the need to incorporate incompatible alkyl and perfluoroalkyl chain units into successful gelators of this class: neither 2 nor 5 wt % concentrations of the nearly perfluorinated amide, $F(CF_2)_7CONHCH_2(CF_2)_7F$ (mp 115.6−116.5 °C), gelates *any* of the liquids in Table 1.

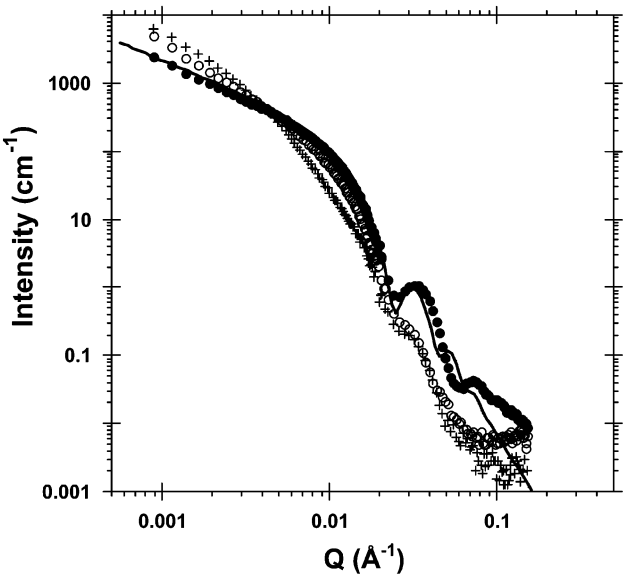

Figure 11. SANS intensity versus Q curves of **4d** organogels in benzene-d_6 at 1 wt % (+) and 2 wt % (○) and in 1-butanol-d_{10} at 2 wt % (●). The full line is the theoretical curve for fibers with circular cross-sections, $r_0 =$ 165 Å.

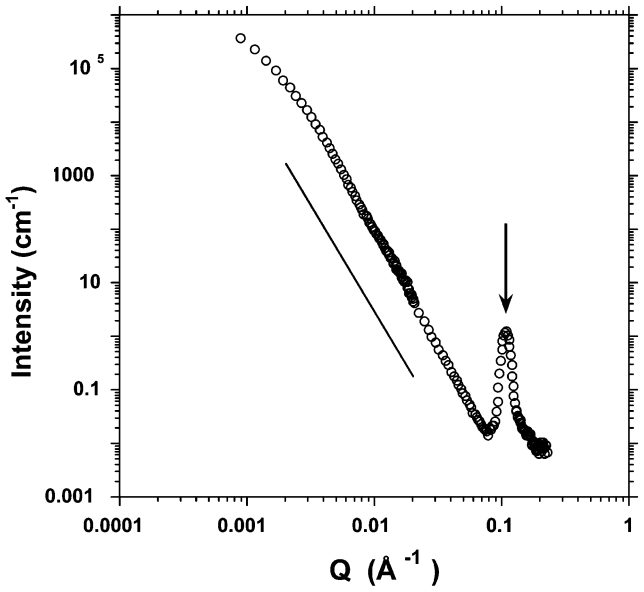

Figure 12. Intensity (I) versus Q profile of a 4 wt % **3c** organogel in 1-butanol-d_{10}. A reference slope −4 is shown, and the arrow points to the Bragg peak ($Q = 0.105$ Å^{-1}).

The cross-sectional dimensions of the *N*-alkyl perfluoroalkanamide fibrils in several liquids are very small (in the nanoscale range), and gels that appear transparent even under POM (N.B., **4c**−**f** and **5** in silicone oil) are obtained. SANS studies show thicker bundles of fibrils for **3c** than for **4d** in gels of both 1-butanol-d_{10} and benzene-d_6. The SANS scattering profiles of organogels of **4d** in benzene-d_6 and in 1-butanol-d_{10} are very different. **4d** fibers exhibit strikingly monodisperse cross-sections in 1-butanol-d_{10} (radius $r = 165$ Å) while in benzene-d_6 the fibers appear associated in more complex aggregates (bundles) that affect the scattering profile as a function of the concentration. By contrast, networks of the organogels of **3c** are polydisperse and more crystalline. In addition, their networks exhibit none of the concentration and solvent dependence found with the gels of **4d**. Finally, the **3c** molecules are periodically packed in planes separated by ca. 58−59 Å according to SANS and X-ray measurements.

Somewhat surprisingly, molecular packing is the same within the neat solid phase and the fibrils of the silicone oil gel of each amide or ester LMOG; all appear to be lamellar. When the aliphatic chain of a perfluorododecanamide **4** contains ≥8 carbon atoms, the lamellar separation distance d changes from being near one to approximately 1.5 times the calculated extended length of the molecules. Clearly, the packing arrangement depends on the alkyl chain length to a large extent as well.

Both the thermal and temporal stabilities of the gels are very dependent on the nature of the gelator aggregates. When the lamellar thickness of the aggregates corresponds to ca. 1.5 times the extended molecular length of the secondary amides, as in **3c** and **4g**, the gels are less stable than when d is near the extended molecular length. An exception to this generalization is **4b** gels (whose lamellar thickness is slightly less than the extended length) in which hydrophobic interactions between the interdigitated shorter alkyl chains (Figure 10b) may not be sufficient to stabilize the aggregates.

The gelating ability of the LMOGs depends on the length of both the alkyl and perfluoroalkyl chains. Within the **4a**−**g** series, the gelating ability increases with increasing alkyl chain length up to four carbon atoms and decreases thereafter. A similar effect is observed when the perfluoroalkyl chain length is varied and the alkyl length is constant, as in **3a**, **4c**, and **5**. The shorter amide **3a** is a poor LMOG (it was able to gelate only *n*-perfluorooctane below room temperature), while gels with the longer amide **5** possess very high thermal and temporal stabilities in alcohols and in *n*-perfluorooctane. To the best of our knowledge, this is the first report of LMOGs that gelate a perfluorinated *n*-alkane. As a result, these systems may be useful for several applications in lithography[54] and even to disperse fire retardants.[55]

Acknowledgment. We thank Dr. Veeradej Chynwat for technical assistance. Financial support to the Georgetown group from the U.S. National Science Foundation and the Petroleum Research Fund (administered by the American Chemical Society) is greatly acknowledged. We also acknowledge the CNRS for a binational travel grant to P.T.

Supporting Information Available: Spectroscopic and analytical data of **3**−**6**, plot showing the dependence of T_g on concentration of **4d** gels in silicone oil, and XRD patterns of several gels and neat powder samples (PDF). This material is available free of charge via the Internet at http://pubs.acs.org.

JA0362407

(54) (a) Schmaljohann, D.; Bae, Y. C.; Weibel, G. L.; Hamad, A. H.; Ober, C. K. *Proc. SPIE-Int. Soc. Opt. Eng.* **2000**, *3999*, 330−334. (b) Bae, Y. C.; Dai, J.; Weibel, G. L.; Ober, C. K. *Polym. Prepr. (Am. Chem. Soc., Div. Polym. Chem.)* **2000**, *41*, 1586−1587. (c) Schmaljohann, D.; Bae, Y. C.; Dai, J.; Weibel, G. L.; Hamad, A. H.; Ober, C. K. *J. Photopolym. Sci. Technol.* **2000**, *13*, 451−458. (d) Bae, Y. C.; Ober, C. K. *Polym. Prepr. (Am. Chem. Soc., Div. Polym. Chem.)* **2001**, *42*, 403−404. (e) Bae, Y. C.; Douki, K.; Yu, T.; Dai, J.; Schmaljohann, D.; Koerner, H.; Ober, C. K. *Chem. Mater.* **2002**, *14*, 1306−1313.

(55) (a) *Fluorinated Surfactants: Synthesis, Properties, and Applications*; Kissa, E., Ed.; Marcel Dekker: New York, 1994. (b) Moody, C. A.; Kwan, W. C.; Martin, J. W.; Muir, D. C. G.; Mabury, S. A. *Anal. Chem.* **2001**, *73*, 2200−2206.